

Using Remote Sensing and Gis Technique to Study Soil Physical Properties for Hour Al-Hammar (South of Iraq)

Aseel Abbas* & Dr. Abdul Razzak T.Ziboon*

Received on:10/2/2009

Accepted on:4/6/2009

Abstract

This paper includes the digital image processing (image enhancement and the digital classification techniques) using ERDAS, ver.,8.7, package for Landsat 7 (ETM+), 3-visible bands with resolution (14.25m), acquired in March 2004 .

The field investigation includes GPS surveying, which coincides with the reports of the laboratory tests (physical tests), which include soil classification test (according to the unified soil classification system (USCS), for certain locations), and spectral measurements by using radiometer instrument.

The main results of this study show that the selected visible bands in the digital visual interpretation process are considered an optimum means to sense the soil types. It is found that the study region soil has high content of the fine soil texture (clay and silt). Therefore, the digital map of unsupervised classification gives good presentation of some of the main landcover classes and merges the others, whereas the supervised classification gives good presentation of the main landcover classes with overall accuracy equal to (99.7%).

Keywords: Studying Spectral Reflectance Measurement and physical Soil properties

توظيف تقنيات التحسس النائي ونظم المعلومات الجغرافية لدراسة الخصائص الفيزيائية لتربة هور الحمار (جنوب العراق) وتأثيرها على الانعكاسية الطيفية

الخلاصة

تم العمل في هذه الدراسة بثلاث مراحل، تضمنت المرحلة الاولى معالجة الصورة الرقمية (تحسين الصورة ، و تقنيات التصنيف الرقمي) بأستخدام الحقيبة البرمجية ERDAS, Ver 8.7/2003 . ومن ثم التحريات الحقلية التي تضمنت عمليات مسح المنطقة بأستخدام جهاز GPS لاخذ احداثيات مواقع اخذ عينات من التربة ومن ثم اجراء الفحوصات المختبرية والتي تتضمن فحوصات فيزيائية للتربة (فحوصات تصنيف التربة تبعا الى نظام تصنيف التربة (USCS)، وبعد ذلك اجراء الفحوصات الطيفية بأستخدام جهاز الراديوميتر وربط نتائج الفحص بنتائج الفحوصات الفيزيائية.

ان اهم الاستنتاجات التي توصلت اليها الدراسة توضح ان الحزم المختارة تعد الامثل في عملية التفسير البصري لتحسس نوع التربة ونسبة الرطوبة، حيث وجد ان تربة منطقة الدراسة يطغي عليها الغرين والطين، كذلك اعطت انطباع عن وجود نسب عالية من المواد العضوية وكذلك وجود نسب من الاملاح في التربة.

ان عملية التصنيف غير الموجه اعطت تمثيل جيد لوصف منطقة الدراسة ووصف اصناف التربة و دمج بعضها بالآخر بينما خارطة التصنيف الموجه اعطت تمثيل جيد لاصناف التربة و بدقة تصنيف = 99.7% .

1. Introduction

Remotely sensed data refer to data of the Earth collected from sensors on satellites or aircraft.

This paper includes three stages. first, field survey, the purpose of field survey was to observe what the different interpretation units are in reality ^[4]. By using GPS instrument (twenty five) samples of soil were obtained from different locations in study region; Table (1) shows the coordinate and states the position of soil samples.

Second, the laboratory tests for the study region soil and analysis results. Many tests were executed to determine some of the physical properties regarding the classification of soils and the effect on the spectral properties of the soil by using multi bands radiometer instrument, at the laboratory of the Soil Mechanics and Sanitary Lab in the University of Technology, and radiometer test.

Third, digital image processing to classify the study region image and the visual interpretation technique results.

Spectral reflectance of soils is determined by their physico-chemical properties, in particular humus content, texture, sulphate, electrical conductivity and water-soluble salts. Moisture content and surface roughness also play an important role ^[3].

2. The Study Area

Al-Hammar marsh selected as study area which is lies south of Euphrates river and extends from Nassriah in the west to Basrah

suburbs at Shatt Alarab in the south of Iraq, about (300)km south of Baghdad. Its length is about 90 km with width is between (25-30) km ^[4].

Locally study region extends between latitude (31°00'-31°30') north and longitude (46°24'-47°18') east, as shown in the fig.(1).

3. Physical Properties Tests

Following are some of the important physical tests, regarding soil classification:-

1. Moisture content
2. Grain Size Distribution
3. Liquid & Plastic Limits

Table (1) shows results of these tests, and Fig.(2) shows sieve & hydrometer curves for some samples and others in (Appendix A)

4. Spectral Reflectance Measurement and Soil properties:

To determine the spectral reflectance for different targets (soil samples) by using multi bands radiometer, the wavelength with its three bands is the same wavelength of the bands 1,2,3 of satellite images, which has the range (0.5-0.6) μm -(0.6-0.7) μm -(0.7-0.8) μm . Fig.(3(a,b,)) shows that the difference in soil properties has apparent effect on spectral reflection curves, so we see in fig.(3.a) that each type of soil has different spectral curve, soil (ML) type has the largest reflection. On the side (CH)soil has the lowest reflection. Fig. (3.b) shows that the increasing

of soil moisture causes decreasing of spectral reflectance curves.

5. Satellite Images Analysis

Many digital processing techniques were carried out to process the satellite image according to the purpose of application. ERDAS software, version 8.7, release 2003, was used to process the digital images.

5.1 Gray Level Histogram

A histogram of gray level content provides a good description of the appearance of an image. The type and degree of enhancement depend on the nature of histogram. Fig (7) shows three bands histogram of merged resolution image of the study area, while table (2) illustrates the statistical parameters of the scene intensity values (DNS). The study of both, figure and table together provides statistical description of study area.

5.2 Image Enhancement

To increase the appearance of the resultant photo map for the image of the study area, two separated processes had be done, as follows :

5.2.1 Convolution Filtering (Edge Enhancement):

The chosen of the suitable kernel matrix filter depends on the purpose of this filter, in this research it was used kernel matrix (7x7) edge enhance to detect the sudden change in gray level from one pixel to another. fig.(5) refers to the edge enhancement convolution filtering to study region image. The features in this image are sharper than those in

the original one, this will facilitate the interpretation of the process required. Fig.(6) shows the gray level histogram for edge enhancements image.

5.2.2 Histogram equalization:

Histogram equalization is a nonlinear stretch, which is one of the radiometric enhancement methods. Fig. (7) shows the histogram equalization results. It develops many features that do not appear to the observer in the original image, it gives useful information for performing image classification successfully, which produces a uniform population density of pixels along the horizontal DN axis that is shown in new gray level histogram after this process in fig. (8).

5.3.2 Supervised Classification.

Following represent the results of supervised classification:

(1) Training Stage:

Six classes are selected in the training stage that represent three land covers classes (water, vegetation and soil) and subclasses of soil types included (CL,SC/SM,CH, and ML) in research region, and the statistical measurements of these classes are computed depending on reflectance value of pixels corresponding to each class versus each of three selected TM bands shown in table (3).

Fig.(10) illustrates the relationship between mean relative reflectance of different classes and Thematic Mapper bands in terms of the spectral response curves.

The spectral response patterns are considered one of the most important results, which give good information and indications about physical and geometric

properties of land cover classes in the research region by means of detailed study, and analysis of spectral response curves of training classes shown in fig.(10) and determination of the factors affecting it by aid of field observation and laboratory and analysis results for the soil samples.

(2) Classification Stages :

The result of classification stage is represented by the map shown in fig.(11). This map is produced by maximum likelihood classifier. Each class is given specific color as well as a number beside this color with summarized explanation. This map includes six classes, which represent the land cover classes in the research region.

5.3.3 Accuracy Assessment

The classification process is not complete until its accuracy is assessed.

The most common means of expressing classification accuracy is a classification error matrix (sometimes called confusion matrix or contingency table). Error matrix compares, on a category-by-category basis, the relationship between known reference data (ground truth) and the corresponding results of an automated classification.

The overall accuracy of supervised classification is (99.7%). The lowest producer's accuracy is (99.22% for "soil (CH)"), it represents a light gray color in supervised classification and the lowest user's accuracy is (96.84% for "soil (CL)") among others due to many interferences which occur between the (CL) soil and other classes, whereas the water class represents the highest accuracy within both accuracies due to clear reflectance which gives its

individuality than other classes. It is important to avoid considering a confusion matrix based on training set values as a measure of overall classification accuracy. The confusion matrix simply tells how well the classifier can classify the training areas and nothing more.

6. Conclusions

1. Differences in surface composition (grain size distribution of soils) and moisture content will effect on the spectral reflectance of soil. So, the amount of moisture held in the surficial soil layer is a function of the soil texture. The finer the soil texture, the greater the soil's ability to maintain high moisture content in the presence of precipitation. The greater the soil moisture, the more incident radiant energy absorbed and the less reflected energy. Therefore, the soil appears darker when wet than when it's dry, in satellite images.

2. Unsupervised classification method is a useful technique to prepare a primitive map for reconnaissance, soil survey, to collect the soil samples and to reduce the effort time and cost.

3. Using high pass filtering convolution enhancement (edge enhancement) is very useful for visual interpretation.

4. Thematic map of soil classification (unsupervised classification) gives good presentation of some classes and merges the others, whereas the supervised classification gives good presentation of the classes with an overall accuracy equal 99.7 %.

5. Using global position system (GPS) in field survey is very essential and important for positioning purposes, and collecting soil samples.

Radiometer is very important for studying the spectral reflectance characteristics for soil. So, its spectral channels are compatible with the same wavelengths that are utilized in the

6. multispectral sensors(TM), (MSS), and (SPOT) to detect the difference in spectral characteristics of soil with respect to the difference of soil types and properties.

7. References

- [1]ASTM,(2002),D422-63,"Standerd Test Method for Particle-size Analysis of soil".
- [2]AL-AHBABY,O.,A.,(2005),"The Use of Remote Sensing and GIS Techniques in Selecting the Best Highway Location for Mosul City". Ph.D, Thesis, University of Technology, Iraq.
- [3].Kerle,N.,etc,(2004), "Principle of Remote Sensing", ITC Educational Textbook series.
- [4].Jensen, J. R., (2000), "Remote Sensing of the Environmental & an

earth sources perspective", university of South Carolina

- [5].Boweles, (1984), "Physical and Geotechnical Properties of Soils", Mc Graw-Hill, Inc
- [6]. Chirico and Epstein, (2000), "Geographic Information System Analysis of Topographic Change in Philadelphia, Pennsylvania During the last Century ", U.S. Geological Survey open File Report, 00-224.
- [7]. Deliback, e.t... (2004), "Reflection values of Saline Soils of Great Mander Basin in Landsat TM images and their statistical Relationships", Agricultural Faculty of Edge University, soil science Dept., Bornova ,35100, Izmir-Turkey
- [8].ERDAS, 8.7, field Guide, 2003.
- [9].Kerle,N.,etc,(2004),"Principle of Remote Sensing", ITC Educational Textbook series.
- [10]. Rolf. A.de.,(2004),"Principle of GIS", ITC Educational Textbook series.

Table (1) Physical Properties of Soil Sample

Sample NO.	Easting	Northing	Moisture content %	Index Properties			Particle Size Distribution & Hydrometer analysis				Name	Description
				LL %	PL %	PI	Clay %	silt %	fine sand %	Gravel %		
648020	3411876	47.81	67.61827	31.57133	36.04694	7	91	2	0	ML	Light gray elastic silty	
648999	3411900	20.14	49.07224	23.07636	25.99588	39	45	5	1	ML	Light brown lean clay	
652251	3410632	20.35	46.05666	25.06663	20.98993	45	44	11	0	CL	Dark sandy silty clay	
655557	3417446	42.14	55.51135	29.55917	25.95111	45	44	11	1	CH	Dark gray lean clay with little sand with shell	
659945	3403745	45.93	47.13514	27.09913	19.90996	30	38	41	1	CL	Dark gray sandy lean clay	
659865	3403333	21.01	42.13821	28.64511	14.05311	36	55	8	0	ML	Light gray elastic silty	
659931	3403393	35.34	47.13514	27.09913	19.90996	30	38	41	1	ML	Brown silty clay	
661574	3403023	14.34	46.29621	28.40777	14.24777	34	48	28	1	ML	Brown sandy silty clay	
661133	3404633	5.22	0	0	NP	8	21	51	0	SC/SM	Clay clayey silty sand	
661144	3404310	11.15	55.51135	29.55917	19.90996	46	3	45	1	CL	Light gray sandy lean clay	
655553	3404189	22.53	53.50445	23.80652	13.65452	30	53	17	0	CL	Clay lean clay with sand	
659859	3404600	33.23	57.57535	22.74631	13.75135	32	31	2	0	CL	Brown lean clay	
648826	3411911	28.91	33.30665	19.30663	15.42835	8	35	47	0	SC/SM	Clay clayey silty sand	
14	649079	3410662	13.4	0	0	NP	17	22	61	0	SC/SM	Dark gray silty sand
15	648925	3410479	25.43	35.21897	25.57437	9.644604	19	56	25	0	ML	Brown clayey sandy silt
16	647857	3412647	19.54	40.99211	22.56581	18.4263	52	37	11	0	CH	Brown sandy silty clay
17	647480	3412890	35.48	57.59888	33.92051	23.67837	50	40	10	0	CH	Brown high plastic silty clay with little sand
18	648273	3411661	43.87	44.67115	24.56038	20.11078	15	76	9	0	CL	Dark gray lean clay
19	648406	3412158	24.68	43.5777	24.23671	19.34098	38	48	14	0	ML	Brown Sandy clayey silt with shells
20	658011	3412059	33.95	52.38568	27.43788	24.94779	10	81	9	0	ML	Light brown silt with little clay & sand
21	657774	341209	37.16	46.79158	24.23469	22.55689	46	42	12	0	CL	Dark gray sandy silty clay
22	657460	3411935	28	37.68759	20.6951	16.99248	44	30	26	0	CL	Brown lean clay
23	656927	3411914	13.88	43.45056	26.66294	16.78762	56	35	9	0	CL	Light gray lean clay with little sand
24	655758	3412273	19.64	41.92062	23.6248	18.29582	39	55	6	0	CL	Brown lean clay
25	654154	3413615	22.35	37.363	21.12116	16.24184	41	46	13	0	CL	Light gray sandy lean clay

Table (2) Statistical Parameters of the satellite Scene of study are

	Band 1	Band 2	Band 3
Mimum (DN)	00	00	00
Maximum	255	255	255
Mean	775.90	771.489	771.634
Median	669	661	662
Mode	770	554	557
Std.Dev.	442.796	440.464	442.758

Table (3) Statistical measurements of training classes that are used in supervised classification.

Class No.	Band 1			
	Min.	Max.	Mean.	S.D
Water	55.00	186.000	96.468	25.625
Vegetation	6.000	32.000	14.663	4.820
Soil(CL)	7.000	46.000	21.620	9.454
Soil(SC/SM)	74.000	105.000	88.942	5.645
Soil(CH)	33.000	151.000	94.152	18.440
Soil(ML)	124.000	225.000	179.625	16.896
Class No.	Band 2			
	Min.	Max.	Mean.	S.D
Water	65.000	199.000	105.972	27.345
Vegetation	30.000	56.000	40.482	5.005
Soil(CL)	12.000	37.000	21.359	4.333
Soil(SC/SM)	52.000	81.000	66.489	5.149
Soil(CH)	17.000	137.000	78.171	19.280
Soil(ML)	124.000	223.000	177.887	17.020
Class No.	Band 3			
	Min.	Max.	Mean.	S.D
Water	84.000	217.000	124.872	28.149
Vegetation	8.000	41.000	17.819	6.266
Soil(CL)	12.000	43.000	22.440	7.072
Soil(SC/SM)	54.000	79.000	66.547	4.729
Soil(CH)	29.000	151.000	90.603	19.074
Soil(ML)	127.000	228.000	180.793	16.938

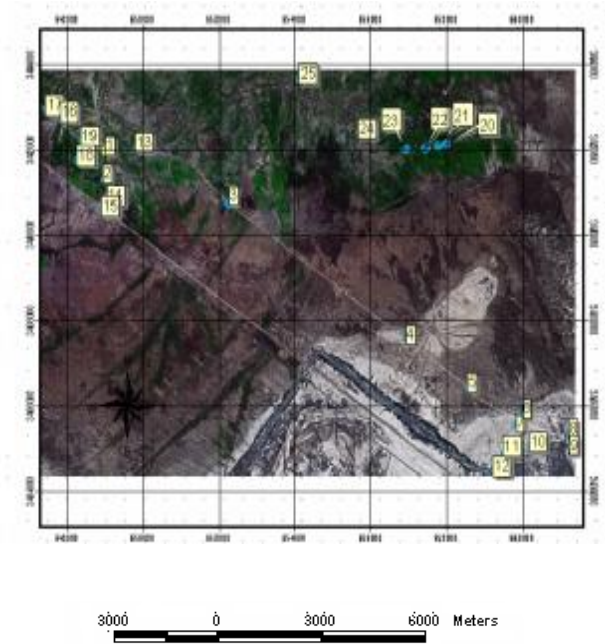
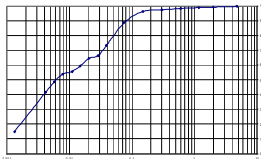
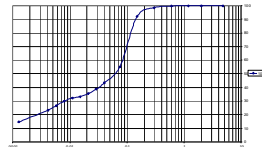


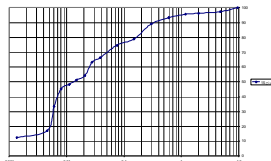
Figure (1) ETM Landsat satellite image show Study Region with points represent soil samples type



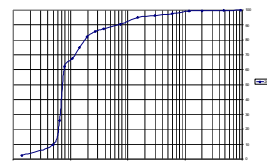
(a) Sample No.(3)



(b) Sample No.(10)



(c) Sample No.(15)



(d) Sample No.(20)

Figure.(2) Results of sieve & hydrometer curves for some samples.

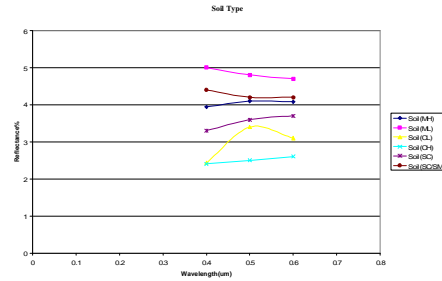


Figure (3.a) Spectral Reflectance curve depend on Soil Type

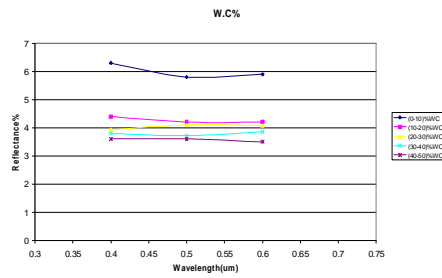


Figure (3.b) Spectral Reflectance curve depend on W.C%

Figure (3,a,b) Difference in Spectral Reflectance due to difference in soil Properties

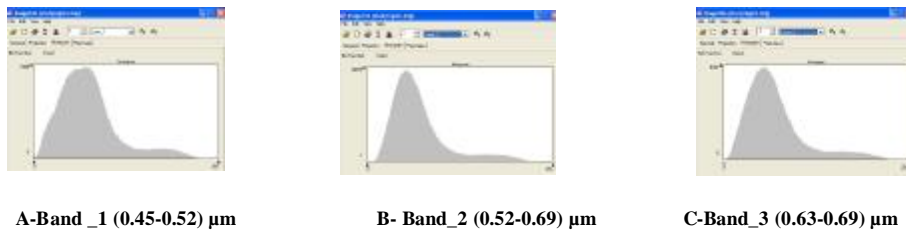


Figure (4) Three bands histogram of a raw image.

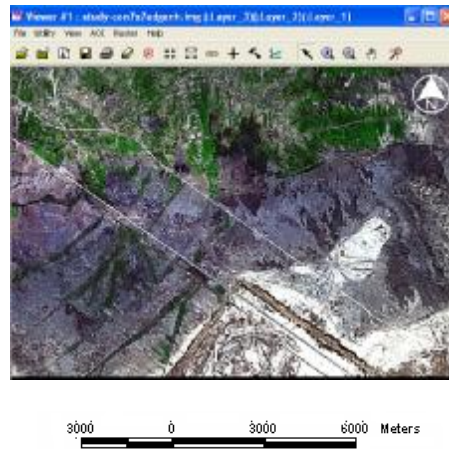


Figure (5) Edge Enhancement for the Study Region Image

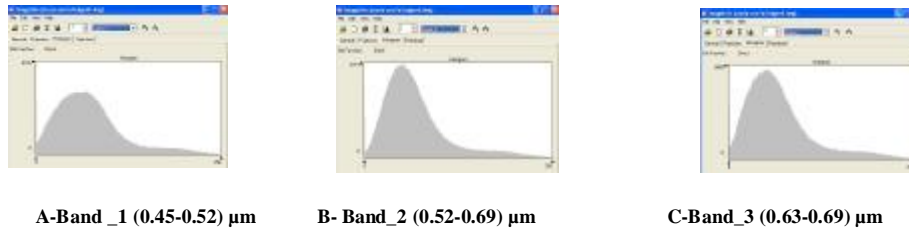


Figure (6) Gray Level Histogram for edge enhancements image

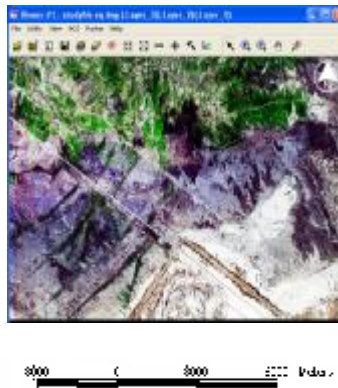


Figure (7) Histogram Equalization process of Study Region

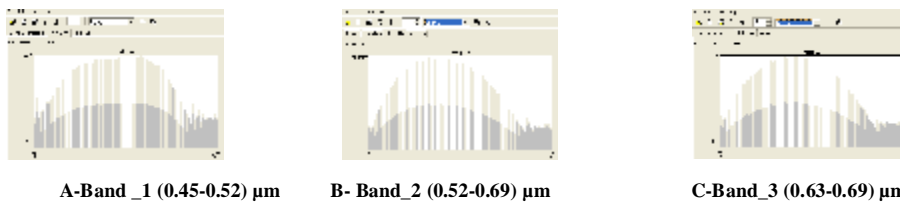


Figure (8) Gray level Histogram after histogram equalization

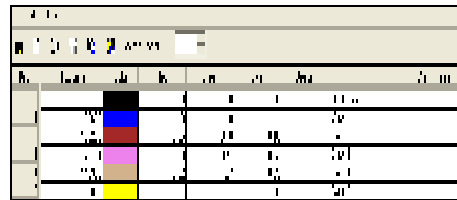
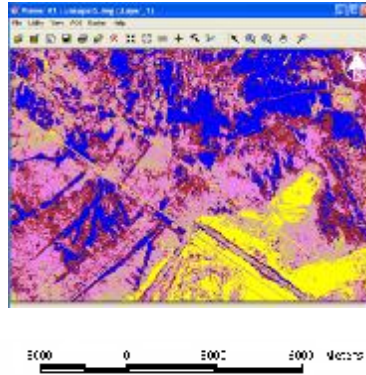


Figure (9) Unsupervised classification image of the study region

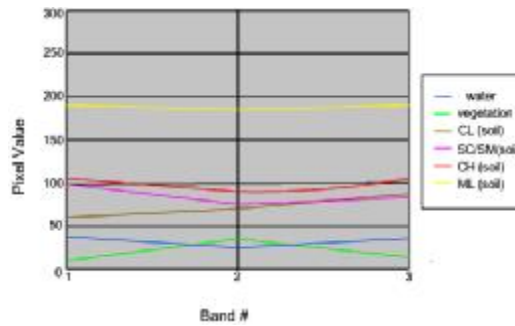


Figure (10) the spectral response curves of land cover classes

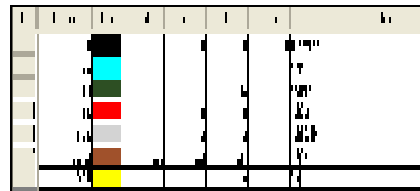
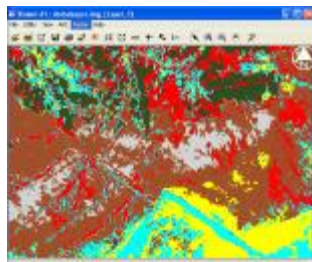
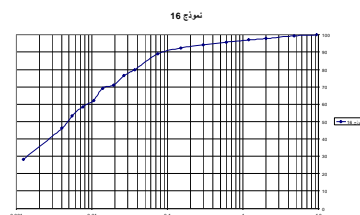
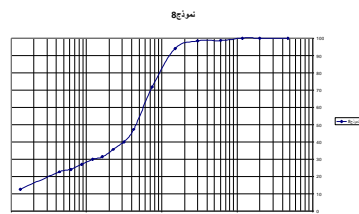
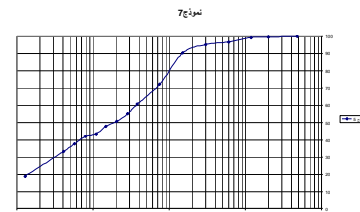
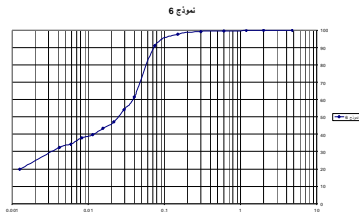
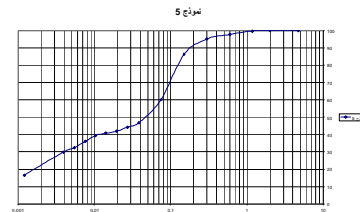
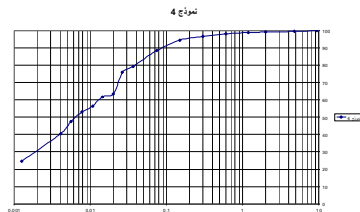
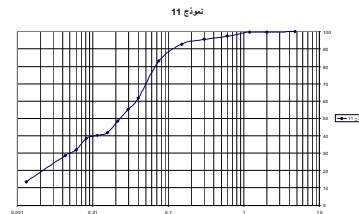
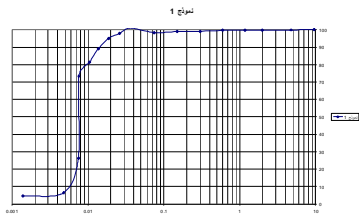
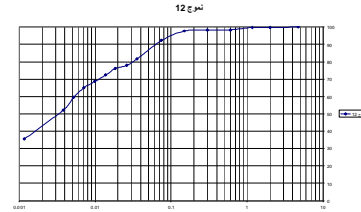
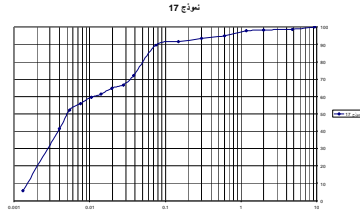
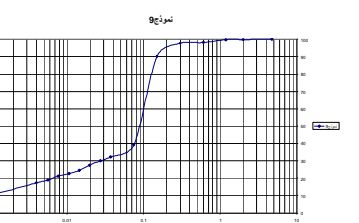
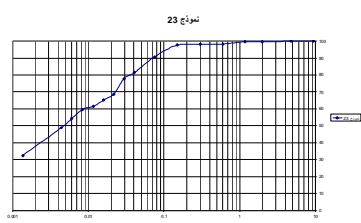
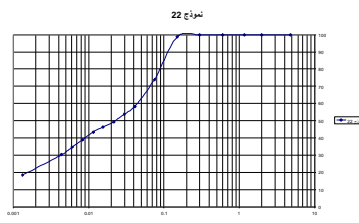
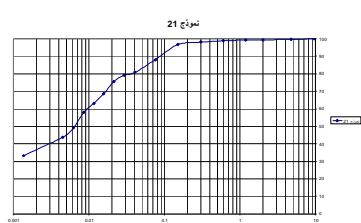
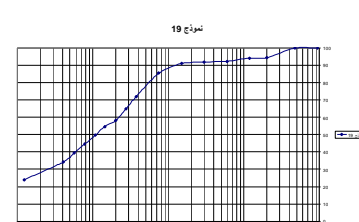
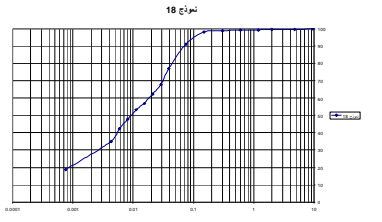
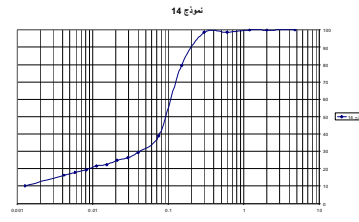
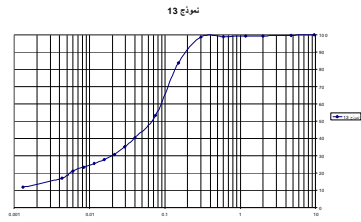


Figure (11) Supervised classification of study region

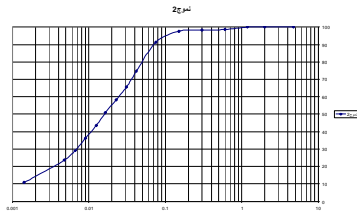
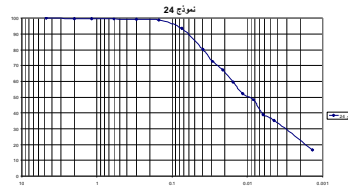
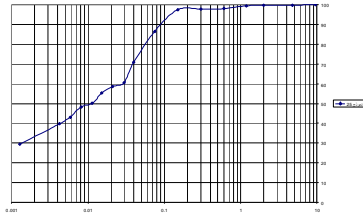
Appendix (A) shows sieve & hydrometer curves for some samples



Appendix (A) shows sieve & hydrometer curves for some samples



Appendix (A) shows sieve & hydrometer curves for some samples



Appendix B

- Refer to "Appendix A: Math Topics" for information on the mean vector and covariance matrix.

Divergence

The formula for computing Divergence (D_{ij}) is as follows:

$$D_{ij} = \frac{1}{2} \text{tr}((C_i - C_j)(C_i^{-1} - C_j^{-1})) + \frac{1}{2} \text{tr}((C_i^{-1} - C_j^{-1})(\mu_i - \mu_j)(\mu_i - \mu_j)^T)$$

Jeffries-Matusita Distance

The formula for computing Jeffries-Matusita Distance (JM) is as follows:

$$\alpha = \frac{1}{8} (\mu_i - \mu_j)^T \left(\frac{C_i + C_j}{2} \right)^{-1} (\mu_i - \mu_j) + \frac{1}{2} \ln \left(\frac{|(C_i + C_j)/2|}{\sqrt{|C_i| \times |C_j|}} \right) ,$$

$$JM_{ij} = \sqrt{2(1 - e^{-\alpha})}$$

Where:

- i and j = the two signatures (classes) being compared
- C_i = the covariance matrix of signature i
- μ_i = the mean vector of signature i
- \ln = the natural logarithm function
- $|C_i|$ = the determinant of C_i (matrix algebra)

Source: Swain and Davis 1978

According to Jensen, "The JM distance has a saturating behavior with increasing class separation like transformed divergence. However, it is not as computationally efficient as transformed divergence" (Jensen 1996).

Separability

Both transformed divergence and Jeffries-Matusita distance have upper and lower bounds. If the calculated divergence is equal to the appropriate upper bound, then the signatures can be said to be totally separable in the bands being studied. A calculated divergence of zero means that the signatures are inseparable.

- TD is between 0 and 2000.
- JM is between 0 and 1414.

A separability listing is a report of the computed divergence for every class pair and one band combination. The listing contains every divergence value for the bands studied for every possible pair of signatures.

The separability listing also contains the average divergence and the minimum divergence for the band set. These numbers can be compared to other separability listings (for other band combinations), to determine which set of bands is the most useful for classification.

Weight Factors

As with the Bayesian classifier (explained below with maximum likelihood), weight factors may be specified for each signature. These weight factors are based on *a priori* probabilities that any given pixel is assigned to each class. For example, if you know that twice as many pixels should be assigned to Class A as to Class B, then Class A should receive a weight factor that is twice that of Class B.

NOTE: The weight factors do not influence the divergence equations (for TD or JM), but they do influence the report of the best average and best minimum separability.

The weight factors for each signature are used to compute a weighted divergence with the following calculation:

$$w_{ij} = \frac{\sum_{i=1}^{c-1} \left(\sum_{j=i+1}^c f_i f_j U_{ij} \right)}{\frac{1}{2} \left[\left(\sum_{i=1}^c f_i \right)^2 - \sum_{i=1}^c f_i^2 \right]}$$

Where:

i and j = the two signatures (classes) being compared

U_{ij} = the unweighted divergence between i and j

W_{ij} = the weighted divergence between i and j

c = the number of signatures (classes)

f_i = the weight factor for signature i

Probability of Error

The Jeffries-Matusita distance is related to the pairwise probability of error, which is the probability that a pixel assigned to class i is actually in class j . Within a range, this probability can be estimated according to the expression below:

$$\frac{1}{16}(2 - JM_{ij}^2)^2 \leq P_e \leq 1 - \frac{1}{2}\left(1 + \frac{1}{2}JM_{ij}^2\right)$$

Where:

i and j = the signatures (classes) being compared

JM_{ij} = the Jeffries-Matusita distance between i and j

P_e = the probability that a pixel is misclassified from i to j

Source: Swain and Davis 1978